ELECTRONICS AND ELECTRICAL ENGINEERING
ISSN 1392 – 1215 2011. No. 9(115)
ELEKTRONIKA IR ELEKTROTECHNIKA

ELECTRICAL ENGINEERING
T 190
ELEKTROS INŽINERIJA

Magnetic Analysis of Modified-Rotor Switched Reluctance Motor

A. Kakilli
Department Of Electrical Education, Marmara University,
Goztepe Campus, Kadikoy, Istanbu, Turkey, phone: +90 216 3365770, e-mail: kakilli@marmara.edu.tr

crossref http://dx.doi.org/10.5755/j01.eee.115.9.742

Introduction

Switched Reluctance Motor (SRM) was used in 1838 in Scotland for the first time as a locomotive motor. Although this motor's basic working principle variable reluctance motor theory had been known before, it was started to be used for variable and adjustable speed applications merely after 1980's. In recent years, through the technological progress of power electronic materials appropriate opportunities have been supplied for the use of this motor. SRM is structurally very base. It has salient poles both at its rotor and stator. Excitation windings are placed only on stator poles. Their being base and lasting, highly efficient are the most important advantage of them. Although a lot studies have been done on them by academicians, their use in the fields of application is not widespread [1–4].

There are many surveys on SRM in literature: Moellem and Ong have realized torque prediction of SRM in their survey using finite elements method. Garrigan and colleagues have observed radial forces in SRMs in their survey. Fenercioğlu and Tarımer have searched the factors affecting phase inductance of SRM. Tang and colleagues have made the transience analysis of SRM under constant and variable speed to evaluate the motor's electromagnetic force and noise. Sundaram and colleagues using finite elements method have made comparative magnetic analysis of different polar surface SRMs. Gizlier and colleagues have observed simulation and magnetic features of SRM by using finite elements method [2, 5–9].

In this paper, rotor pole of a 12/8-pole SRM have been modified by helical method without changing its geometry, magnetic analyses have been made separately as flat rotor and modified rotor with Ansoft Maxwell 3D, the results have been evaluated comparatively .

Switched reluctance motor electrical equivalent circuit

SRM is structurally the simplest of all electrical motors. There is no winding or magnet on the rotor of SRM. There are only excitation windings on stators. Due to these properties SRM's electrical equivalent circuit is very base. In this motor phase inductance is dependent on the position of the rotor and magnitude of the current passing through the stator winding. Single phase equivalent circuit is given below in Fig. 1. [10, 11].

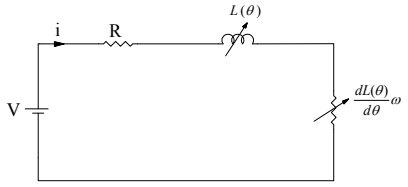

Fig. 1. Single phase equivalent circuit

SRM's voltage per phase is given in (1)

$$V = Ri + \frac{d\psi(\theta, i)}{dt} - M(\theta)\frac{di'}{dt}, \quad (1)$$

here V – source voltage, R – a phase winding resistance of stator, ψ – magnetic flux, I – single phase current of stator, $M(\theta)$ – mutual inductance, θ – rotor bearing, i' – current of the winding just before the phase excited in stator. By ignoring the mutual inductance of the phases in SRM magnetic flux can be expressed as in (2) [10–12]

$$\psi = L(\theta, i). \quad (2)$$

By reorganizing expression in (1) according to (2), can be written as

$$V = Ri + \frac{dL(\theta, i)}{dt} - M(\theta)\frac{di'}{dt}, \quad (3)$$

here $L(\theta,i)$ is phase inductance. By making the necessary operations phase voltage in (4) is obtained in this expression

$$V = Ri + L(\theta)\frac{d(i)}{dt} - i\frac{dL(\theta)}{dt}. \quad (4)$$

By ignoring mutual inductance in (4)

$$\frac{dL(\theta, i)}{dt} = \frac{dL(\theta, i)}{d\theta}\omega \quad (5)$$

is obtained (ω is angular velocity).

When these expressions are simplified

$$V = Ri + L(\theta)\frac{d(i)}{d\theta}\omega + i\frac{dL(\theta)}{d\theta}\omega\,, \qquad (6)$$

SRM's phase inductance is obtained [11].

Magnetic model of SRM

In a 3-phase, 12/8 pole SRM, magnetic flux of current passing through phase windings loop the circuits via stator yoke, stator poles, air gaps, rotor poles and rotor yoke. Maximum passage of flux takes place at overlapping positions. In an overlapping position stator and rotor are face to face, at θ=0°. In Fig. 2. magnetic flux through stator and rotor of a 12/8 pole SRM in an overlapping position is shown. In this motor, at a full overlapping state inductance is maximum whereas, when there is no overlapping inductance is minimum. Because of this, SRM is switched on in area between the beginning state of overlapping and full state of overlapping by phase excitation. When this state is obtained phase 1 excitation is aborted and phase 2 is excited [2].

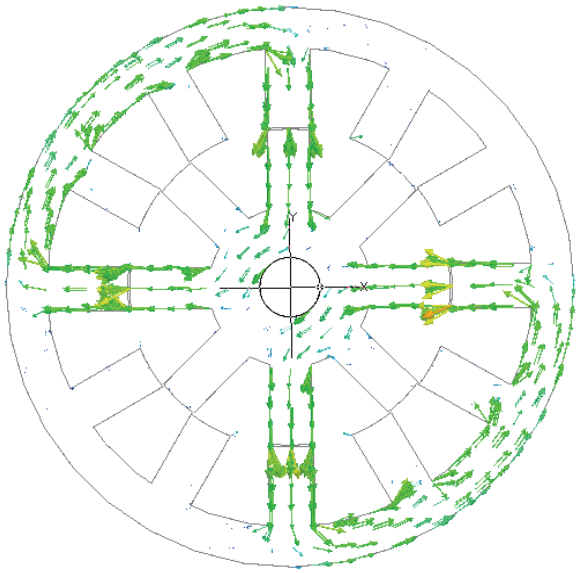

Fig. 2. Magnetic flux through stator and rotor of a 12/8 pole SRM in an overlapping position

Magnetic equivalent circuit obtained related to the flux path of SRM in an overlapping position is shown in Fig. 3., parameters and related definitions are presented in Table 1.

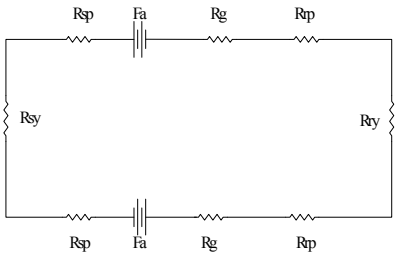

Fig. 3.12/8 pole SRM 's magnetic equivalent circuit

Table 1. Magnetic equivalent circuit parameters

Symbol	Explanation
Fa	mmf of a single phase winding (At)
Rsp	Stator pole reluctance (H^{-1})
Rrp	Rotor pole reluctance (H^{-1})
Rsy	Stator yoke reluctance(H^{-1})
Rry	Rotor yoke reluctance (H^{-1})
Rg	Air gap reluctance (H^{-1})

In order to analyze the magnetic circuit total mmf and reluctance should be known. Here, total mmf for a single base is calculated according to (7)

$$\sum F = 2Fa\,. \qquad (7)$$

Total reluctance of a SRM is related to the rotor angle. Total reluctance expression of the equivalent circuit in Fig. 3 obtained for overlapping position is given in (8)

$$R = 2(R_g + R_{sp} + R_{rp}) + R_{sy} + R_{ry}\,. \qquad (8)$$

When reluctance unknowns are expanded

$$R = 2\left[\left(\frac{l_g}{\mu_0 A_g}\right) + \left(\frac{l_{sp}}{\mu_0\mu_r A_{sp}}\right) + \left(\frac{l_{rp}}{\mu_0\mu_r A_{rp}}\right)\right] + \left(\frac{l_{sy}}{\mu_0\mu_r A_{sy}}\right) + \left(\frac{l_{ry}}{\mu_0\mu_r A_{ry}}\right)\,, \qquad (9)$$

expression is obtained. Here R – total reluctance, l_g – air gap length, l_{sp} – stator pole length, l_{rp} – rotor pole length, l_{sy} – stator yoke length, l_{ry} – rotor yoke length, μ_0 – gap magnetic permeability, μ_r – relative magnetic permeability. By using total reluctance, inductance can be calculated by

$$L = \frac{N^2}{R}\,, \qquad (10)$$

here N is the number of a single phase winding. Determining maximum and minimum inductance in SRMs is related to flux path. By using maximum inductance predicted from the overlapping state and minimum inductance predicted during a magnetic analysis with a specific rotor angle, inductances at middle rotor angles can be calculated. SRM has low energy ratio. In order to describe this, energy conversion period is calculated magnetically. Inductance in this motor is expressed in harmonic 1 in Fourier series in relation with the position of rotor. Inductance and bond flux are given respectively with (11) and (12) [13]:

$$L(\theta, i) = [a_0 - a_1 Cos(n_R\theta)]\,, \qquad (11)$$

$$\lambda(\theta, i) = [a_0 - a_1 Cos(n_R\theta)]i\,. \qquad (12)$$

a_0 and a_1 coefficients can be calculated as:

$$a_0 = \frac{1}{2}(L_a + L_u), \qquad (13)$$

$$a_1 = \frac{1}{2}(L_a - L_u), \qquad (14)$$

here θ– angular rotor position, n_R – rotor pole number, L_a –

maximum inductance per phase, L_u – minimum inductance per phase. SRM's electromagnetic torque expression is given in (15)

$$T_e = \sum_{j=1}^{m} \frac{1}{2} i_j^2 \frac{dL_j(\theta, i)}{d\theta}, \qquad (15)$$

here *Te* – total moment produced in SRM, *j* – phase index, *m* – phase number.

Application

In this paper a 3-phase 12/8 pole SRM is used. Table 2 shows electrical and geometrical parameters of the SRM chosen.

Table 2. Electrical and geometrical parameters of SRM

Symbol	Explanation	Dimension
Rri	Rotor apothem (m)	0.040
Rro	Rotor radius (m)	0.079
Rsi	Stator apothem (m)	0.120
Rso	Stator radius (m)	0.140
ly	Stator yoke length (m)	0.224
lg	Air gap (m)	0.001
lstk	Packet length (m)	0.100
n_s	Stator pole number	12
n_r	Rotor pole number	8
q	Phase number	3
N	Winding number per phase	200

In Ansoft Maxwell/3D Simulator related to the parameters given in Table 2 firstly 12/8 pole base structure rotor SRM's geometrical model is obtained. Fig. 4 shows the dimensional model of SRM realized in a Simulator.

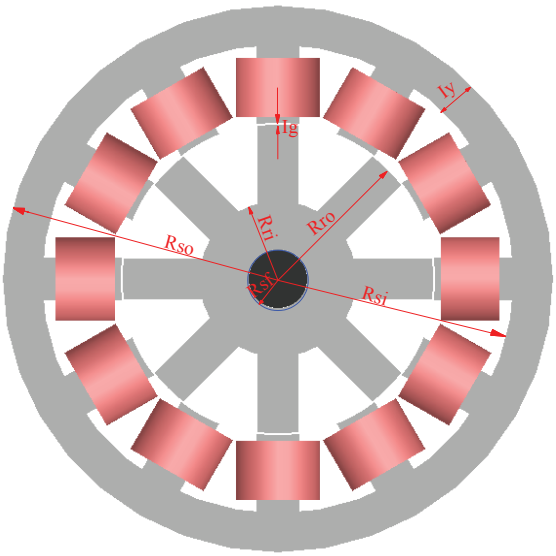

Fig. 4. Geometrical model of 12/8 pole SRM

Steel 1010 is chosen as metal sheet of stator and rotor cores to define the material in design. B-H curve which gives the structural characteristic of this material is shown in Fig. 5.

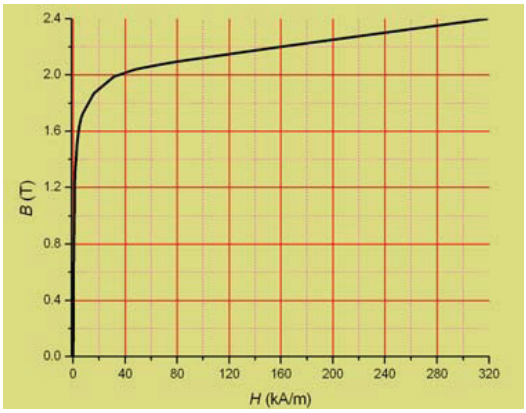

Fig. 5. Steel B-H curve of 1010 [2]

In the surveys held, secondly motor is modeled again by distorting rotor pole structure base rotor structure SRM at 3.6° angles. In Fig. 6.a 3.6° modified, 6.b base forms of rotor are shown.

Evaluations made over the results obtained by the analysis using finite elements method by winding rotors of SRMs having 12/8 pole modified and base rotor geometry clockwise and counter-clockwise at 0°, 3°, 6° , 9° , 12°, 15° , 18°, -22.5° (Fig. 6).

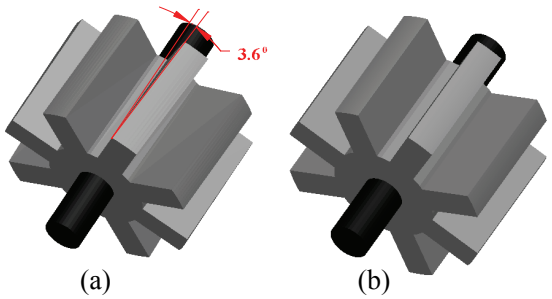

Fig. 6. Base and modified models designed for SRM

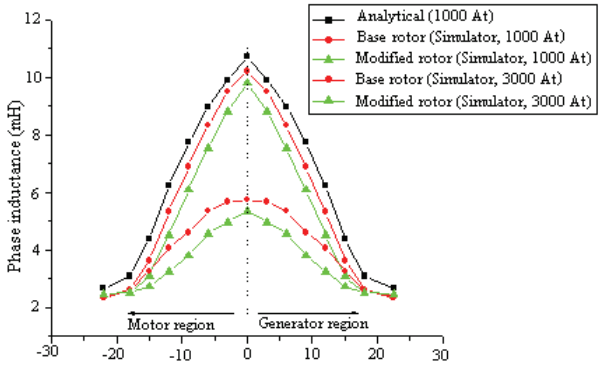

Fig. 7. Phase inductance graphics related to modified and base rotor structured

In Fig. 7. phase inductance graphics of SRMs having different geometry for two different loading state related to rotor positions are shown. Overlapping takes place between the ranges for motor to work $-15^\circ \le \theta \le 0^\circ$ and for generator to work $0^\circ \le \theta \le 15^\circ$ to excite the related phases of SRM.

An area beyond this range is the part where there is no overlapping and phase winding flux should be cut. Analytical calculations and results obtained from the Simulator are approximately close to each other.

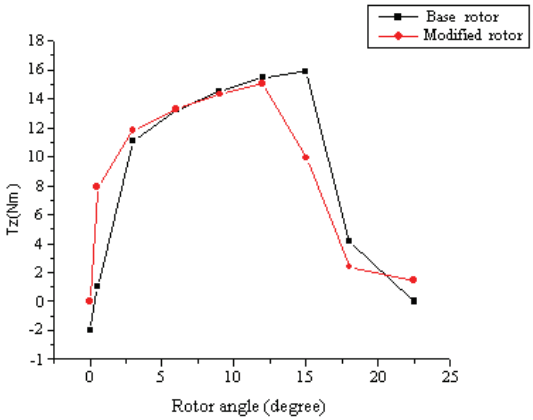

Fig. 8. Torque graphics at shaft axis related to rotor positions of modified and base SRMs (1000At)

In the state of 1000At loading, since B-H curve in Fig. 5 is in unsaturated region, phase inductance takes 10.8mH value as a result of magnetic permeability (B/H) curve, which determines phase inductance at this point, being high, in the state of 3000 At loading, since B-H curve's magnetic permeability is lower due to it's being in saturated region and phase inductance value is 5.8 mH.

In Fig. 8. torque graphics at shaft axis related to rotor positions of modified and base SRMs are seen. As it will be seen from these graphics, torque production in a modified rotor structured SRM takes place in a larger field than a base structured SRM. Besides, torque fluctuations are less in modified structured SRMs.

For the full overlapping state in Fig. 9.a modified rotor, Fig. 9.b base rotor SRM's magnetic flux density (B) vectors in stator and rotor core at 10A phase excitation are seen. Maximum *B* on the surface of stator and rotor cores in modified rotor structured SRM is 1.7 T, whereas in base rotor structured SRM maximum *B* is 1.8 T. Also, in figures given for both kinds, it is observed that magnetic circuits are fully developed without a leakage flux.

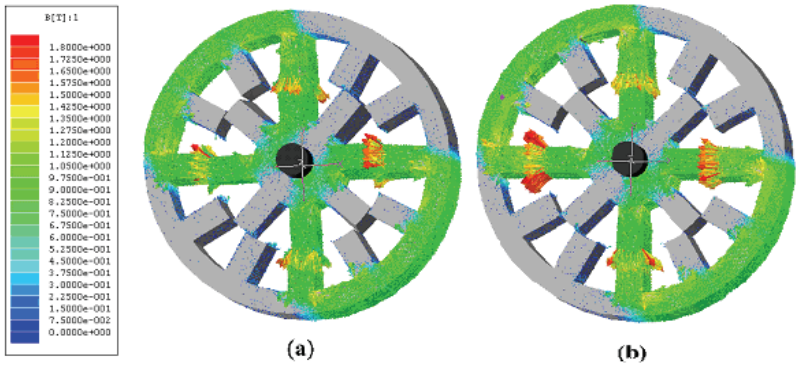

Fig. 9. At full overlapping state,.(a)modified rotor,.(b) base rotor SRMs magnetic flux vectors in stator and rotor kernels at phase excitation flux of 3A (1000At)

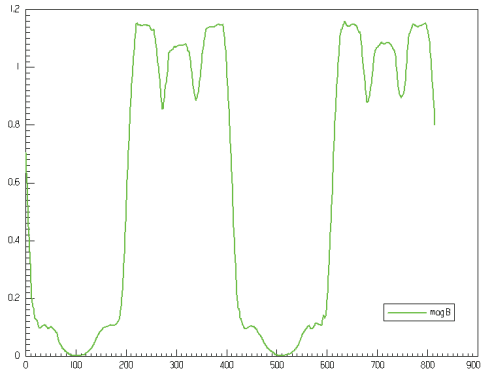

Fig. 10. Graphic of magnetic flux density received from a contour placed into a stator yoke (1000At)

In Fig. 10 graphic of magnetic flux density received from a contour of 359^0 placed into a stator yoke is seen. In the range of 200-450mm in the stator yoke 1st magnetic circuit, in the range of 600-850mm 2nd magnetic circuit have comprised. Saggings at the points 250, 350, 650 and 750 mm of the graphic point at the stator poles inside the 1st and 2nd magnetic circuits and show that there is no leakage flux over the poles.

In Fig. 11. Magnetic flux density distributions on (a) modified rotor, (b) base rotor SRM's stator and rotor core surfaces at full overlapping $\theta=0^o$ position are seen. It is seen that maximum B for both a and b figures is 1.8 T and saturation has started at coincidence part of the stator and rotor poles.

While this condition can be observed in all polar arc regions of stator and rotor in base rotor SRM, it can be observed only in one of the corners of polar arc regions of stator and rotor where they meet in modified motor structured SRM.

In Fig. 12 are shown magnetic flux density distributions on (a) modified rotor, (b) base rotor SRM's stator and rotor kernel surfaces at the beginning of overlapping $\theta=15^o$ positions are seen. It is seen that maximum B for both a and b figures is 1.8 T and saturation has taken place at the starting point of overlapping in the corners of polar arc regions. The reason is that there happen constrictions at this point while passing from stator to rotor.

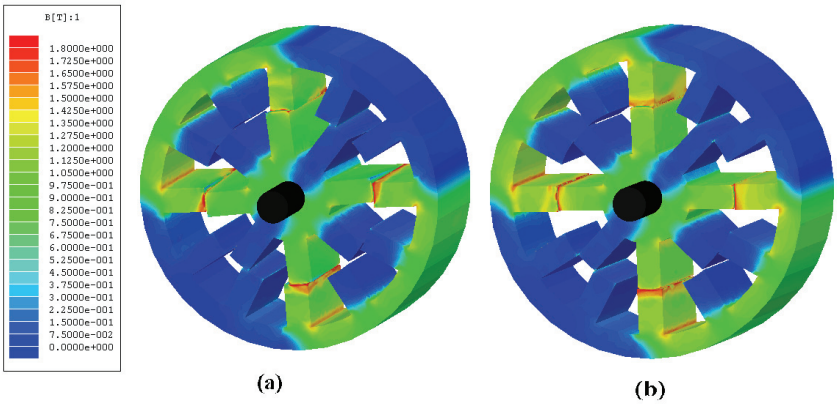

Fig. 11. Magnetic flux density distribution on (a) modified rotor, (b) base rotor SRM's stator and rotor kernel surfaces at overlapping position (1000 At, $\theta=0^{o}$)

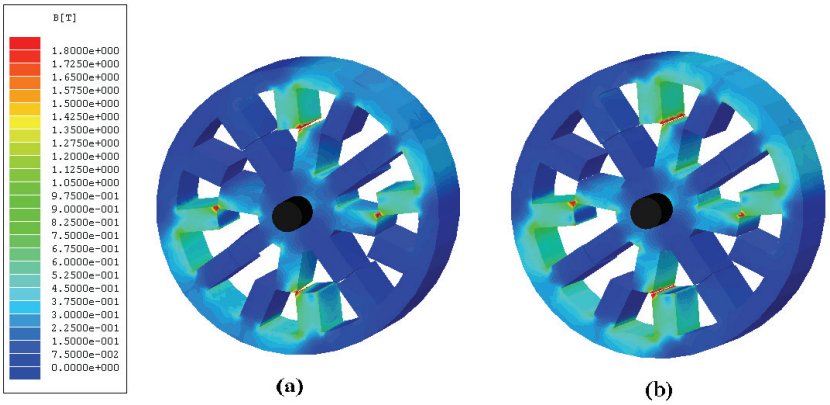

Fig. 12. Magnetic flux density distribution on (a) modified rotor, (b) base rotor SRM's stator and rotor kernel surfaces at overlapping position (1000 At, $\theta=15^{o}$)

Conclusions

Since parameters like inductance and power change according to rotor position, magnetic material structure, etc., it is difficult to determine SRM's electrical and magnetic characteristics using analytical methods. Because of this, simulations applications which coincide with analytical results are preferred in design works.

It is possible to obtain torque production in larger fields with geometric designs made by changing rotor modified without changing the geometry of stator and appropriate magnetic field distributions on rotor surfaces. Besides, torque fluctuations and acoustic noise can be reduced.

Acknowledgments

The author would like to thank the editor and the reviewers for their constructive comments and suggestions. Also would like to thank Zafer Doğan for valuable contribution.

References

1. **Miller T. J. E.** Switched Reluctance Motors and Their Control. – Magna Physics Publishing, Oxford, 1993.
2. **Fenercioglu A.** Desing and Mangetically Analysis of Circular Flux Linear Actuator // Electronics and Electrical Engineering. – Kaunas: Technologija, 2010. – No. 5(101). – P. 21–23.
3. **Iqbal H., Hossain S. A.,** Modeling, simulation, and control of switched reluctance motor drives // IEEE Trans. Ind. Electronics, 2005. – No. 52(6). – P. 1625–1634.
4. **Omaç Z., Kürüm H., Selçuk A. H.** 18/12 Kutuplu Bir Anahtarlı Relüktans Motorun Tasarımı, İncelenmesi ve Kontrolü // Fırat Üniv. Fen ve Müh. Bil. Dergisi, 2007. – No. 19(3). – P. 339–346.
5. **Moellem M., Ong C. M.** Predicting the Torque of Switched Reluctance Machine from Its Finite Element Field Solition // IEEE Tran. On Energy Conversion, 1990. – No. 5. – P. 733–739.
6. **Garrigan N. R., Soong W. L., Stephens C. M., Storace A., Lipo T. A.** Radial force characteristics of a switched reluctance machine // IEEE Industry Applications Conference, 1999. – No. 4. – P. 2250–2258.
7. **Tang Z., Pillay P., Chen Y., Omekanda A. M.** Prediction of electromagnetic forces and vibrations in SRMs operating at steady–state and transient speeds // IEEE Trans. Ind. Application, 2005. – No. 41(4). – P. 927–937.
8. **Sundaram M., Navaneethan P., Vasanthakumar M.** Magnetic Analysis and Comparison of Switched Reluctance Motor with Different Stator Pole Shapes Using a 3D Finite Element Method // ICGST–ACSE Journal, 2009. – No. 9(2).
9. **Gizlier E., Güngör S., Erfan F., Mergen A. F.** Investigatıon of magnetic charaterıstics and simulation of switched reluctance motor usıng fem analysıs // The 2th International Conference on Elrctrical and Electronics Engineering (ELECO'2001), 2001.

10. **Bal G.** Özel Elektrik Makinaları. – Seçkin Yayınevi, Ankara, 2004. – 195 p.
11. **Dursun M., Saygın A.** Günes Enerjisi ile Çalısan Bir Sulama Sistemi için Boost Konvertörlü Anahtarlamalı Relüktans Motor Sürücüsü // Erciyes Üniversitesi Fen Bilimleri Ens. Dergisi, 2006. – No. 22(1–2). – P. 57–65.
12. **Krishnan R.** Switched Reluctance Motor Drives. – CRC Press, Florida, 2001. – 169 p.
13. **Fenercioğlu A.** Anahtarlamalı Relüktans Motorun (HY–ARM) Tasarımı ve Analizi. – Doktora Tezi, Gazi Üniversitesi Fen Bilimleri Enstitüsü, 2006.

Received 2010 12 21
Accepted after revision 2011 03 21

A. Kakilli. Magnetic Analysis of Modified-Rotor Switched Reluctance Motor // Electronics and Electrical Engineering. – Kaunas: Technologija, 2011. – No. 9(115). – P. 21–26.

In this study magnetic analyses of a 3-phase, 12/8-pole, modified-rotor switched reluctance motor have been made. For this purpose, this motor has been modeled distorting 3.6 degrees by using a rotor helical method having a right geometry in 3-D environment, using the finite element method with Ansoft-Maxwell 3D, magnetic analyses of it have been made. The results of this analysis have been compared with the results calculated by analytical methods. The results obtained through the studies have been given modally. Ill. 12, bibl. 13, tabl. 2 (in English; abstracts in English and Lithuanian).

A. Kakilli. Reluktacinio variklio su modifikuotu rotoriumi magnetinė analizė // Elektronika ir elektrotechnika. – Kaunas: Technologija, 2011. – Nr. 9(115). – P. 21–26.

Atlikta trifazio 12/8 polių reluktacinio variklio su modifikuotu rotoriumi magnetinė analizė. Šis variklis buvo modeliuojamas pakreipiant 3,6 laipsnio ir taikant spiralinį rotoriaus metodą, kuriam būdinga taisyklinga geometrija 3D aplinkoje. Taikant baigtinių elementų metodą, pagal „Ansoft-Maxwell 3D“ programą atlikta šio variklio magnetinė analizė. Analizės rezultatai palyginti su analitiškai gautais skaičiavimų rezultatais. Il. 12, bibl. 13, lent. 2 (anglų kalba; santraukos anglų ir lietuvių k.).